Resonant two-photon ionization spectroscopy of jet-cooled OsC

Olha Krechkivska and Michael D. Morse[a)]
Department of Chemistry, University of Utah, Salt Lake City, Utah 84112, USA

(Received 25 July 2007; accepted 30 November 2007; published online 29 February 2008)

The optical spectrum of diatomic OsC has been investigated for the first time, with transitions recorded in the range from 17 390 to 22 990 cm^{-1}. Six bands were rotationally resolved and analyzed to obtain ground and excited state rotational constants and bond lengths. Spectra for six OsC isotopomers, $^{192}Os^{12}C$ (40.3% natural abundance), $^{190}Os^{12}C$(26.0%), $^{189}Os^{12}C$(16.0%), $^{188}Os^{12}C$(13.1%), $^{187}Os^{12}C$(1.9%), and $^{186}Os^{12}C$(1.6%), were recorded and rotationally analyzed. The ground state was found to be $X\,^3\Delta_3$, deriving from the $4\delta^3 16\sigma^1$ electronic configuration. Four bands were found to originate from the $X\,^3\Delta_3$ ground state, giving $B_0''=0.533\,492(33)$ cm^{-1} and $r_0''=1.672\,67(5)$ Å for the $^{192}Os^{12}C$ isotopomer (1σ error limits); two of these, the 0-0[19.1]2 $\leftarrow X\,^3\Delta_3$ and 1-0[19.1]2$\leftarrow X\,^3\Delta_3$ bands, form a vibrational progression with $\Delta G'_{1/2}=953.019$ cm^{-1}. The remaining two bands were identified as originating from an $\Omega''=0$ level that remains populated in the supersonic expansion. This level is assigned as the low-lying $A\,^3\Sigma^-_{0+}$ state, which derives from the $4\delta^2 16\sigma^2$ electronic configuration. The OsC molecule differs from the isovalent RuC molecule in having an $X\,^3\Delta_3$ ground state, rather than the $X\,2\delta^4$, $^1\Sigma^+$ ground state found in RuC. This difference in electronic structure is due to the relativistic stabilization of the 6*s* orbital in Os, an effect which favors occupation of the 6*s*-like 16σ orbital. The relativistic stabilization of the 16σ orbital also lowers the energy of the $4\delta^2 16\sigma^2$, $^3\Sigma^-$ term, allowing this term to remain populated in the supersonically cooled molecular beam. © *2008 American Institute of Physics*. [DOI: 10.1063/1.2827482]

I. INTRODUCTION

Recently there has been considerable interest in studying transition metal carbides due to their significance in homogeneous and heterogeneous catalysis, organometallic chemistry, and biological processes. Among the transition metal monocarbides, the 3*d* and 4*d* series have been more extensively studied than the 5*d* series, both experimentally and theoretically. Because a review of all current work on transition metal carbides is not the purpose of this article, we will concentrate on the 5*d* transition metal monocarbides.

Experimental data on the 5*d* transition metal carbides are scarce, with spectra available only for WC,[1,2] IrC,[3–6] and PtC.[7–14] Bond dissociation energies have been measured using Knudsen effusion mass spectrometry for OsC,[15,16] IrC,[17,18] and PtC,[19] and an upper bound on the bond energy of HfC has been established by this method.[20] Bond dissociation energies of the 5*d* transition metal monocarbide cations WC^+,[21] ReC^+,[22] IrC^+,[23] and PtC^+ (Ref. 24) have also been measured using guided ion beam collision induced dissociation techniques. Theoretical studies have been published on TaC,[25] WC,[26] OsC,[16] IrC,[27] PtC,[28] and AuC^+.[29] As compared to the 3*d* and 4*d* series, theoretical studies of the 5*d* transition metal carbides are very challenging due to the increasing importance of relativistic effects (including spin-orbit coupling) and electron correlation.

No spectroscopic studies on diatomic OsC have been previously reported. Thermochemical measurements of the bond dissociation energy have been performed by Gingerich and co-workers using the Knudsen effusion method, thereby providing a bond energy of 6.28 ± 0.15 eV (605.6 ± 14.0 kJ/mol).[15,16] In addition, Meloni *et al.* reported *ab initio* calculations on the $S=0$, 1, 2, and 3 spin states of diatomic OsC at various levels of theory.[16] They find that the ordering of states changes significantly depending on the level of theory employed. At the highest level used in their study, the CCSD(T) level of theory, the lowest energy state was found to be $^3\Sigma^-$, arising from the $4\delta^2 16\sigma^2$ electronic configuration. The $^3\Delta$ state arising from the $4\delta^3 16\sigma^1$ electronic configuration was calculated to lie 0.28 eV (2220 cm^{-1}) above the $^3\Sigma^-$ state. In a more recent investigation, the B3LYP density functional theory was applied to OsC, along with the other 5*d* transition metal monocarbides.[30] Again, the $^3\Sigma^-$ state was predicted to be the ground state, with a bond length of 1.674 Å. Neither computational investigation of OsC included spin-orbit effects, however, although the authors of the B3LYP density functional study noted that the results may be different when these are considered.

Previously published experimental studies on the other group 8 transition metal carbides, FeC (Refs. 31–34) and RuC (Refs. 35–39) reveal their ground states to be $^3\Delta_3$ for FeC, arising from the $9\sigma^1 1\delta^3$ configuration and $^1\Sigma^+$ for RuC, arising from the $2\delta^4$ electronic configuration. The much greater importance of relativistic and spin-orbit effects in OsC makes this molecule an interesting point of comparison. If the relativistic stabilization of the 6*s* orbital is sufficient, the $4\delta^2 16\sigma^2$, $^3\Sigma^-(0^+)$ state may be the ground state, as predicted by *ab initio* calculations. If not, it is likely that the

a)Electronic mail: morse@chem.utah.edu. FAX: (801)-581-8433

 © 2008 American Institute of Physics

Author complimentary copy. Redistribution subject to AIP license or copyright, see http://jcp.aip.org/jcp/copyright.jsp

$4\delta^3 16\sigma^1$, $^3\Delta_3$ state will emerge as the ground level. Given the relativistic stabilization of the 6*s*-like 16σ orbital, it is unlikely that the ground state will be the $4\delta^4$, $^1\Sigma^+$ state that is the analog of the ground state of RuC.

The spectroscopic results obtained in the present study demonstrate that the ground level of the OsC molecule is indeed the $4\delta^3 16\sigma^1$, $^3\Delta_3$ state. Much weaker transitions arising from a state with $\Omega=0$ are also observed, and these are assigned to the low-lying $A\,^3\Sigma^-(0^+)$ state, which remains populated in the supersonic beam.

II. EXPERIMENTAL

In this work, diatomic OsC was investigated using resonant two-photon ionization (R2PI) spectroscopy. The apparatus used in the present study has been previously described.[33] In brief, it consists of two vacuum chambers; the first of which contains the pulsed supersonic nozzle, rotating and translating target disk mount, and molecular beam skimmer (1 cm diameter, 50° inside angle), and is pumped by a VHS-10 diffusion pump, backed by a KDH-130 rotary mechanical pump. These experiments were conducted under conditions in which the ion gauge reading was in the range of $(5-8)\times10^{-5}$ and $(1-2)\times10^{-6}$ Torr in the first and second chambers, respectively. The OsC molecules were produced by laser ablation of a 45:55 mole ratio vanadium:osmium alloy disk [Nd:YAG (yttrium aluminum garnet) laser, 355 nm, 12–15 mJ/pulse], with the laser timed to coincide with the carrier gas pulse. Helium seeded with approximately 3% methane was used as the carrier gas. A backing pressure of 50 psi (gauge) was found to be optimal for producing diatomic OsC. The OsC signal was so strong that it was possible to collect rotationally resolved spectra of the strongest vibrational transitions for the minor isotopomers (^{187}Os^{12}C and ^{186}Os^{12}C, with 1.94% and 1.57% natural abundance, respectively).

The second chamber is evacuated by an Edwards 160 diffusion pump, backed by a Welch 1397 rotary mechanical pump. It houses a reflectron-type time-of-flight mass spectrometer with Wiley-McLaren ion source optics.[40,41] The molecular beam was exposed to the output of a Nd:YAG-pumped tunable dye laser counterpropagating along the axis of the molecular beam and was crossed at right angles by the output of an ArF excimer laser (193 nm) about 40 ns later in time. Molecules that absorb the dye laser radiation are then ionized by the excimer radiation, so that the ion signal of the molecule of interest may be monitored as a function of the dye laser frequency to provide the optical spectrum.

To investigate the vibronically resolved spectrum of OsC, the dye laser was scanned in low resolution mode (0.15 cm^{-1}) using an output energy of 3–7 mJ/pulse. To reveal rotational structure within the vibrational transitions, an intracavity étalon was inserted into the oscillator cavity, which was then pressure scanned with sulfur hexafluoride (SF_6), giving a resolution of 0.04 cm^{-1}. In this mode, the dye laser gave about 1 mJ of output energy, which was filtered even further to reduce power broadening. During pressure scans, the pressure in the dye laser cavity was varied from 30 to 800 Torr, allowing continuous scans of about 15 cm^{-1}.

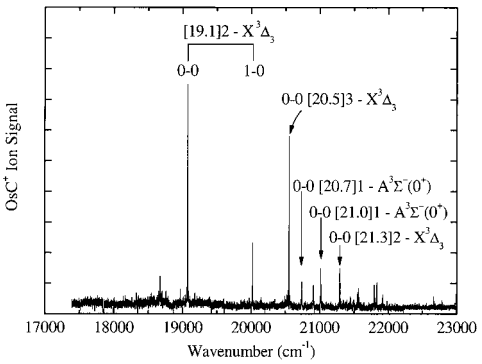

FIG. 1. Vibronically resolved resonant two-photon ionization spectrum of OsC over the range of 17 390–22 990 cm^{-1}.

For each high resolution spectrum a reference spectrum of I_2 (Refs. 42 and 43) or Te_2 (Refs. 44 and 45) (for vibrational bands below and above 20 000 cm^{-1}, respectively) was collected for calibration purposes. As the OsC molecules were traveling toward the light source at the beam velocity of helium (1.77×10^5 cm s^{-1}), all measured line positions were shifted by a small amount (0.11–0.12 cm^{-1}) to correct for the Doppler shift.

For each rotationally resolved vibrational transition, the excited state lifetime was measured. For this purpose, the dye laser was set to excite the transition and the ion signal intensity was monitored as a function of the dye laser-excimer delay. The data were then fitted to an exponential decay curve using the Marquardt nonlinear least-squares algorithm.[46] To provide estimates of the error in the lifetime measurement, three independent measurements of the lifetime were made, and the standard deviation among the three values is reported.

III. RESULTS

A. Low resolution spectrum of OsC

The vibronically resolved spectrum of OsC, collected between 17 390 and 22 990 cm^{-1}, is presented in Fig. 1. Approximately 11 vibrational bands of various intensities are observed over the spectral range of 19 000–22 000 cm^{-1}, and the strongest six of these were rotationally resolved. In this region only one vibrational progression is observed, which is identified as the $[19.1]2\leftarrow X\,^3\Delta_3$ system on the basis of rotationally resolved studies described below. Here the notation [19.1]2 refers to an $\Omega'=2$ excited electronic state with its $v=0$ level lying approximately 19.1×10^3 cm^{-1} above the ground level. The rotationally resolved bands give fitted band origins, from which the vibrational interval is deduced to be $\Delta G'_{1/2}=953.0189\pm0.0022$ cm^{-1} for the most abundant isotopomer, ^{192}Os^{12}C. Here and throughout this article, 1σ error limits are provided. The assignment of the two bands of this system to a common band system is supported by their similar upper state rotational constants (0.519 and 0.511 cm^{-1}), and the consistency of the measured isotope shifts with their assignment as 0-0 and 1-0 bands.

For the remaining transitions, no obvious vibrational progression could be identified, so all information about these band systems comes from the rotationally resolved

Author complimentary copy. Redistribution subject to AIP license or copyright, see http://jcp.aip.org/jcp/copyright.jsp

TABLE I. Upper state parameters of OsC: band origins (cm^{-1}). rotational constants B' (cm^{-1}). upper state bond lengths (Å). and lifetime (μs).

Molecule		0–0 $[19.1]2 \leftarrow X\,^3\Delta_3$	1–0 $[19.1]2 \leftarrow X\,^3\Delta_3$	0–0 $[20.5]3 \leftarrow X\,^3\Delta_3$	0–0 $[20.7]1 \leftarrow A\,^3\Sigma^-_{0+}$	0–0 $[21.0]1 \leftarrow A\,^3\Sigma^-_{0+}$	0–0 $[21.2]2 \leftarrow X\,^3\Delta_3$
$^{186}Os^{12}C$	ν_0	19 063.948 2(49)	20 018.167 6(19)	20 543.230 5(32)			21 284.169 3(41)
	B'	0.520 993(146)	0.512 105(150)	0.525 856(65)			0.490 873(66)
	r'	1.694 23(24)	1.708 86(25)	1.686 37(10)			1.745 43(12)
$^{187}Os^{12}C$	ν_0	19 063.898 5(45)	20 017.917 7(52)	20 543.197 7(27)			21 284.035 8(31)
	B'	0.520 506(125)	0.512 185(211)	0.525 748(102)			0.490 039(203)
	r'	1.694 74(20)	1.708 45(35)	1.686 27(16)			1.746 63(36)
$^{188}Os^{12}C$	ν_0	19 063.868 3(20)	20 017.676 9(13)	20 543.169 4(22)	20 729.267 0(53)	21 006.256 6(25)	21 283.978 1(27)
	B'	0.520 378(44)	0.511 580(40)	0.525 619(30)	0.477 964(286)	0.488 509(227)	0.490 239(35)
	r'	1.694 68(7)	1.709 19(7)	1.686 21(5)	1.768 27(53)	1.749 08(41)	1.745 99(6)
$^{189}Os^{12}C$	ν_0	19 063.857 3(36)	20 017.452 7(48)	20 543.165 4(19)	20 729.163 6(25)	21 006.222 9(17)	21 283.890 1(22)
	B'	0.519 969(79)	0.511 469(90)	0.525 491(81)	0.478 249(136)	0.488 382(116)	0.490 194(131)
	r'	1.695 07(13)	1.709 10(15)	1.686 14(13)	1.767 46(25)	1.749 03(21)	1.745 80(23)
$^{190}Os^{12}C$	ν_0	19 063.792 4(21)	20 017.200 3(18)	20 543.115 2(25)	20 729.046 2(35)	21 006.161 4(27)	21 283.783 7(13)
	B'	0.519 744(45)	0.510 974(47)	0.525 046(43)	0.478 086(193)	0.488 155(182)	0.489 729(47)
	r'	1.695 17(7)	1.709 66(8)	1.686 59(7)	1.767 49(36)	1.749 16(33)	1.746 35(8)
$^{192}Os^{12}C$	ν_0	19 063.718 4(16)	20 016.737 3(15)	20 543.073 6(15)	20 728.835 9(16)	21 006.073 4(14)	21 283.594 1(13)
	B'	0.519 497(34)	0.510 669(33)	0.524 808(34)	0.477 612(84)	0.487 908(77)	0.489 490(31)
	r'	1.695 05(6)	1.709 64(6)	1.686 45(6)	1.767 82(16)	1.749 06(14)	1.746 24(6)
Lifetime (μs)		0.228(41)	0.307(19)	0.160(14)	0.496(21)	0.350(59)	0.340(16)

work, which is described below. Excited state lifetimes, band origins, and upper state rotational constants for all of the measured bands are provided in Table I. Fitted lower state rotational constants and bond lengths obtained by inversion of these data are provided in Table II. In all cases, bands originating from the same lower level were used in a combined fit, so that the most precise spectroscopic parameters could be obtained. Line positions for all of the rotationally resolved bands for all of the interpretable isotopomers of OsC have been deposited with the Electronic Physics Auxiliary Publication Service (EPAPS) of the American Institute of Physics[47] and are also available from the author (M.D.M.). The electronic document also contains spectra for all of the rotationally resolved bands.

TABLE II. Spectroscopic constants for the $X\,^3\Delta_3$ and $A\,^3\Sigma^-_{0+}$ states of OsC.

Molecule		$X\,^3\Delta_3$	$A\,^3\Sigma^-_{0+}$
$^{186}Os^{12}C$	B_0'' (cm^{-1})	0.534 821(99)	
	r_0'' (Å)	1.672 18(16)	
$^{187}Os^{12}C$	B_0'' (cm^{-1})	0.534 495(104)	
	r_0'' (Å)	1.672 42(16)	
$^{188}Os^{12}C$	B_0'' (cm^{-1})	0.534 313(43)	0.518 212(219)
	r_0'' (Å)	1.672 43(7)	1.698 22(36)
$^{189}Os^{12}C$	B_0'' (cm^{-1})	0.534 360(63)	0.518 268(121)
	r_0'' (Å)	1.672 09(9)	1.697 85(20)
$^{190}Os^{12}C$	B_0'' (cm^{-1})	0.533 730(44)	0.517 922(196)
	r_0'' (Å)	1.672 82(7)	1.698 15(32)
$^{192}Os^{12}C$	B_0'' (cm^{-1})	0.533 492(33)	0.517 713(91)
	r_0'' (Å)	1.672 67(5)	1.697 97(15)

B. Rotationally resolved spectra

1. The $[19.1]2 \leftarrow X\,^3\Delta_3$ band system of OsC

This system consists of two strong bands, with the origin band lying near 19 064 cm^{-1} and the 1-0 band near 20 017 cm^{-1}; no transitions to higher vibrational levels were detected. The two upper levels have short lifetimes of 228 ± 41 and 307 ± 19 ns. Because of the strength of these transitions, and the relative ease of producing OsC in the supersonic expansion, it was possible to record rotationally resolved spectra for all of the OsC isotopomers having greater than 1% natural abundance: $^{192}Os^{12}C$ (40.3% natural abundance), $^{190}Os^{12}C$(26.0%), $^{189}Os^{12}C$(16.0%), $^{188}Os^{12}C$(13.1%), $^{187}Os^{12}C$(1.94%), and $^{186}Os^{12}C$(1.57%). All rotational lines were successfully fitted to the equation

$$\upsilon = \upsilon_0 + B'J'(J'+1) - B''J''(J''+1), \tag{3.1}$$

allowing upper and lower state rotational constants and Ω values to be extracted. Spectroscopic constants, bond lengths, and lifetimes for the 0-0 and 1 -0 bands are presented in Tables I and II. Figure 2 displays the rotationally resolved spectrum of the 0-0 band of the $[19.1]2 \leftarrow X\,^3\Delta_3$ system for the most abundant isotopomer, $^{192}Os^{12}C$.

When the spectrum was first collected, the P lines appeared much stronger than the R lines, consistent with the Hönl-London factors for a $\Delta\Omega = -1$ transition. This is not evident in the spectrum displayed in Fig. 2 because during the scan over the R branch the dye laser intensity was increased to bring out the weaker lines. The observation of first lines of $R(3)$, $Q(3)$, and $P(3)$ provides $\Omega'' = 3$, $\Omega' = 2$, confirming the Hönl-London prediction of a $\Delta\Omega = -1$ transition. As can be seen from the spectrum, the lines in the R and P

Author complimentary copy. Redistribution subject to AIP license or copyright, see http://jcp.aip.org/jcp/copyright.jsp

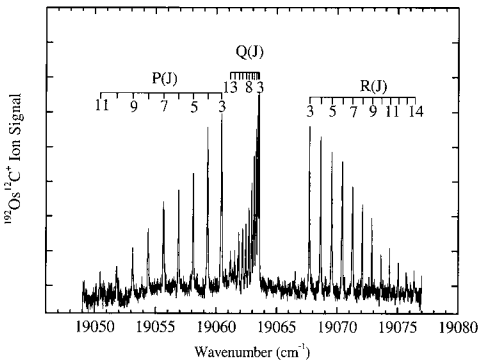

FIG. 2. Rotationally resolved scan over the 0-0 band of the [19.1]2 $\leftarrow X\,^3\Delta_3$ system of $^{192}Os^{12}C$.

branches fan out nearly symmetrically, without formation of a band head. The Q lines are closely spaced and fan out to lower energy, indicating that the bond length increases slightly upon electronic excitation. If sufficient population were present in the high J levels, a band head would eventually form in the R branch. There are large gaps between first Q line and first P and R lines, indicative of the high values of Ω in the upper and lower states. The isotope shift between the lightest ($^{186}Os^{12}C$) and the heaviest ($^{192}Os^{12}C$) isotopomers is only 0.2298 cm^{-1}, indicating that this is vibrationally a 0-0 band.

The 1-0 band possesses rotationally resolved structure very similar to that in Fig. 2, except that Q lines fan out more rapidly to the red. The isotope shift between $^{186}Os^{12}C$ and $^{192}Os^{12}C$ was found to be 1.4303 cm^{-1}, which is consistent with the 1-0 vibrational assignment.

2. The [20.5]3 $\leftarrow X\,^3\Delta_3$ band system of OsC

A bit further to the blue, another strong transition was found near 20 543 cm^{-1}, for which it was again possible to collect rotationally resolved and assignable spectra for all of the OsC isotopomers with greater than 1% natural abundance. Figure 3 displays the rotationally resolved spectrum of this feature for $^{192}Os^{12}C$, which we identify as the 0-0 band of the [20.5]3 $\leftarrow X\,^3\Delta_3$ system. Again, the lines in the P and R branches fan out nearly symmetrically without formation of a band head. The large gaps between the Q branch and the first P and R lines again indicate that this transition corresponds to high Ω values. The Q lines fan out to lower energy and are very closely spaced. Assignment of the first rotational lines proved that this is an $\Omega'=3\leftarrow\Omega''=3$ transition and originates from the same $\Omega''=3$ level as the bands discussed above. The small isotope shift of 0.1569 cm^{-1} between heaviest and lightest OsC isotopomers indicates that this is a $v'=0\leftarrow v''=0$ band. The bond length changes very slightly upon electronic excitation, only by 0.0138 Å, causing the 1-0 and higher members of the band system to have prohibitively small Franck-Condon factors. Thus, it should come as no surprise that only a single member of this band system is observed.

3. The 20 729 and 21 006 cm^{-1} $\Omega'=1\leftarrow\Omega''=0$ bands of OsC

In the vibronically resolved spectrum displayed in Fig. 1, two weak bands are observed near 20 729 and 21 006 cm^{-1}. The upper states of these features have somewhat longer lifetimes than the other transitions observed in this work, but this is not sufficient to explain their weak intensity in the spectrum. Higher resolution investigations (0.04 cm^{-1}) permitted rotationally resolved spectra to be recorded and analyzed for the four isotopomers of OsC with natural abundances over 10% for both bands. The two bands have quite similar rotational structure, so we present their analysis together, even though they are not apparently members of the same electronic band system.

The rotationally resolved spectrum of the 21 006 cm^{-1} band for $^{192}Os^{12}C$ is presented in Fig. 4. The Q lines are widely spaced and fan out to lower energy. There are no gaps between the Q branch and the P and R branches, immediately demonstrating that the lower state differs from that found in the previously discussed bands. A band head is formed in the R branch, indicating a significant increase in bond length upon electronic excitation. Fitting the rotational lines using Eq. (3.1) provides upper and lower state rotational constants, which are given in Tables I and II, respectively. For both the 20 729 and 21 006 cm^{-1} bands, the first lines are $R(0)$, $Q(1)$, and $P(2)$, which identifies both bands as $\Omega'=1\leftarrow\Omega''=0$ transitions. The assignment of the lower state as the $A\,^3\Sigma^-_{0+}$ state is justified below in the discussion section and is based on molecular orbital arguments together with a comparison to the available *ab initio* calculations. The small isotope shift between the band origins for the $^{188}Os^{12}C$ and

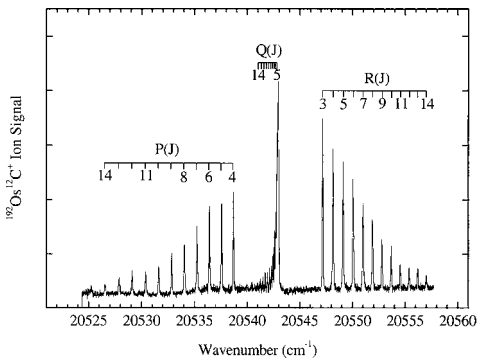

FIG. 3. Rotationally resolved scan over the 0-0 band of the [20.5]3 $\leftarrow X\,^3\Delta_3$ system of $^{192}Os^{12}C$.

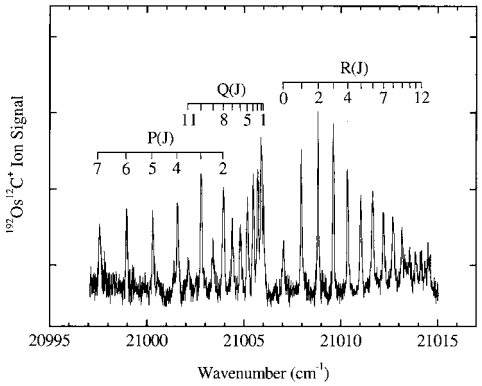

FIG. 4. Rotationally resolved scan over the 0-0 band of the [21.0]1 $\leftarrow A\,^3\Sigma^-_{0+}$ system of $^{192}Os^{12}C$.

Author complimentary copy. Redistribution subject to AIP license or copyright, see http://jcp.aip.org/jcp/copyright.jsp

$^{192}Os^{12}C$ isotopomers, 0.1832 cm^{-1}, suggests that the 21 006 cm^{-1} feature is vibrationally a 0-0 band. Accordingly, this feature is assigned as the 0-0 band of the $[21.0]1 \leftarrow A\ ^3\Sigma_{0+}^-$ band system.

The 20 729 cm^{-1} band is the weaker of the two bands, so while scanning in high resolution mode the dye laser power was increased. As a result, the rotational lines were a bit power broadened comparing to the 21 006 cm^{-1} band, but it was still possible to extract useful information. The rotationally resolved spectrum is very similar to that displayed in Fig. 4, with a band head in the R branch. Again, the first lines are found to be $R(0)$, $Q(1)$, and $P(2)$, establishing the band as another $\Omega'=1 \leftarrow \Omega''=0$ transition. The lower state rotational constant is the same as in the 21 006 cm^{-1} band, allowing both bands to be used in a combined least-squares fit. The small isotope shift between the $^{188}Os^{12}C$ and $^{192}Os^{12}C$ isotopomers, 0.4311 cm^{-1}, is about halfway between what might be expected for a 0-0 band and a 1-0 band, so that vibrational assignment of this single feature is a bit ambiguous. For the purposes of discussion, however, we designate this feature as the 0-0 band of the $[20.7]1 \leftarrow A\ ^3\Sigma_{0+}^-$ band system.

The ^{189}Os atom has nuclear spin, $I=3/2$, but neither the 20 729 nor the 21 006 cm^{-1} band shows significant hyperfine broadening or splitting compared to the other isotopomers. No hyperfine splitting would be expected for the $A\ ^3\Sigma_{0+}^-$ lower state, which is expected to belong to Hund's case (a'_β) due to the large second-order spin-orbit splitting expected in such a state, which causes $\Lambda=0$ and $\Omega=0$ to be good quantum numbers.[48,49] Thus, we may conclude that the hyperfine splitting in the upper states of these transitions is also negligible on the scale of our measurements. In contrast, hyperfine splitting or broadening is obvious in the $^{189}Os^{12}C$ isotopomer in all of the rotationally resolved spectra originating from the $X\ ^3\Delta_3$ state. This is discussed in Sec. III B 5 below.

4. The 21 284 cm^{-1} $\Omega'=2 \leftarrow X\ ^3\Delta_3$ band of OsC

The weak feature found in Fig. 1 near 21 284 cm^{-1} has also been rotationally resolved and analyzed, yielding useful data for all of the isotopomers of OsC with greater than 1% natural abundance. The rotationally resolved spectrum of this band looks very similar to that displayed in Fig. 2, except it has more widely spaced, red-shaded Q and P lines, and more closely spaced R lines leading to an R branch band head at $R(10)$. These facts indicate a significant lengthening of the bond upon electronic excitation. The appearance of the spectrum and subsequent rotational analysis show that this is an $\Omega'=2 \leftarrow \Omega''=3$ transition. The $\nu_0(^{186}Os^{12}C) - \nu_0(^{192}Os^{12}C)$ isotope shift is rather large, 0.5752 cm^{-1}, but because there are no other observed bands with $\Omega'=2$ that fit into a vibrational progression, we tentatively identify the band as the 0-0 vibrational band of the $[21.3]2 \leftarrow X\ ^3\Delta_3$ band system.

5. Hyperfine structure of the rotationally resolved bands

Two of the Os isotopes, ^{187}Os ($I=1/2$, 1.96% natural abundance) and ^{189}Os ($I=3/2$, 16.15%), have nonzero nuclear spin and are therefore subject to hyperfine interactions. The less abundant ^{187}Os isotope has a magnetic moment of 0.0643 nuclear magnetons (n.m.), while the more abundant ^{189}Os has a much larger magnetic moment of 0.6565 n.m.[50] Thus, hyperfine effects are expected to be much more readily observed in $^{189}Os^{12}C$ than in any of the other isotopomers. Indeed, hyperfine splitting and broadening are only evident in our spectra for the $^{189}Os^{12}C$ species.

Hyperfine broadening or splitting is evident in the spectra of $^{189}Os^{12}C$ for all of the bands originating from the $X\ ^3\Delta_3$ level, and for none of the bands originating from the $A\ ^3\Sigma_{0+}^-$ level. Due to the huge spin-orbit parameter for the $5d$ orbitals of Os, $\zeta_{5d}(Os) \approx 3045\ cm^{-1}$,[51] the $X\ ^3\Delta_3$ level is expected to lie approximately 3000 cm^{-1} below the $^3\Delta_2$ level, causing both levels to conform to Hund's case (a_β). Likewise, an estimate of the shift of the $4\delta^2 16\sigma^2$, $A\ ^3\Sigma_{0+}^-$ level due to its spin-orbit perturbation by the higher-lying isoconfigurational $4\delta^2 16\sigma^2$, $^1\Sigma_{0+}^+$ level suggests that the $A\ ^3\Sigma_{0+}^-$ level is lowered in energy by 4000–6000 cm^{-1} due to this effect, causing it to be well separated from the corresponding $A\ ^3\Sigma_1^-$ level, placing the $A\ ^3\Sigma_{0+}^-$ level firmly in Hund's case (a'_β). Given the enormous spin-orbit parameter for Os, it is likely that all of the upper states found for this molecule are also Hund's case (a) states, or spin-orbit induced mixtures of such states. Thus, hyperfine splittings in all of the states of this molecule are expected to follow Hund's case (a_β) formula,

$$E_{hf}(S,\Lambda,\Sigma,\Omega,I,J,F) = h\Omega\left[\frac{F(F+1)-I(I+1)-J(J+1)}{2J(J+1)}\right], \tag{3.2}$$

where

$$h = a\Lambda + \left(b_F + \frac{2}{3}c\right)\Sigma, \tag{3.3}$$

$$a = 2.000 g_I \beta_e \beta_n \langle r^{-3}\rangle, \tag{3.4}$$

$$b_F = g_e g_I \beta_e \beta_n \langle r^{-3}\rangle, \tag{3.5}$$

and

$$c = \tfrac{3}{2} g_e g_I \beta_e \beta_n \langle 3\cos^2\theta - 1\rangle \langle r^{-3}\rangle. \tag{3.6}$$

Here $g_e=2.002\,319\,3$ is the electronic g factor;[50] $g_I \equiv \mu_I/I$ is the nuclear g factor, given by the nuclear magnetic dipole moment in nuclear magnetons divided by the nuclear spin I; β_e is the Bohr magneton; β_n is the nuclear magneton; $|\psi(0)|^2$ is the probability density of finding the electron at the magnetic nucleus; and θ is the angle between the internuclear axis and the vector from the magnetic nucleus to the electron. In these expressions, the expectation values provide averages for a single unpaired electron. In cases in which there are more than one unpaired electron, these formulas must be generalized to include a sum over all unpaired electrons,[49,52]

$$h = \left\langle \sum_i \left[a_i \hat{\ell}_{z,i} + \left(b_{F,i} + \tfrac{2}{3}c_i\right)\hat{s}_{z,i}\right]\right\rangle, \tag{3.7}$$

where the sum is over all electrons outside of closed shells, $\hat{\ell}_{z,i}$ and $\hat{s}_{z,i}$ give the projections of electronic orbital and spin

Author complimentary copy. Redistribution subject to AIP license or copyright, see http://jcp.aip.org/jcp/copyright.jsp

TABLE III. Upper and lower state fitted parameters of $^{189}Os^{12}C$, including hyperfine effect [obtained using the PGOPHER program (Ref. 54)].

Molecule		0–0 $[19.1]2-X\,^3\Delta_3$	1–0 $[19.1]2-X\,^3\Delta_3$	0–0 $[20.5]3-X\,^3\Delta_3$	0–0 $[21.2]2-X\,^3\Delta_3$
$^{189}Os^{12}C$	ν_0 (cm^{-1})	19 062.737	20 016.316	20 543 151	21 282.735
	B'' (cm^{-1})	0.5326	0.5332	0.534 6	0.5346
	r'' (Å)	1.6749	1.6739	1.671 7	1.6717
	h'' (cm^{-1})	0.142	0.1428	0.132	0.1287
	B' (cm^{-1})	0.5193	0.5117	0.524 41	0.4899
	r' (Å)	1.6962	1.7087	1.687 9	1.7463
	h' (cm^{-1})	0.0148	0.0169	−0.007	0.0141

angular momentum along the internuclear axis for electron i, respectively, and the parameters a_i, b_{Fi}, and c_i are given by formulas (3.4)–(3.6), with the expectation values and $|\Psi(0)|^2$ evaluated for electron i.

Büttgenbach has provided a detailed review of hyperfine structure in the $4d$ and $5d$ atoms,[53] including a summary of the results of fitting measured atomic hyperfine levels. For ^{189}Os, Büttgenbach listed the parameters $a^{01}=0.0120\ cm^{-1}$, $a^{12}=0.0051\ cm^{-1}$, $a^{10}_{5d}=-0.0042\ cm^{-1}$, and $a^{10}_{6s}=0.2577\ cm^{-1}$, as averaged values for the $5d^66s^2$ and $5d^76s^1$ configurations. These correspond to values of the a, b_F, and c parameters of $a_\delta=0.0120\ cm^{-1}$, $2/3c_\delta=-0.0029\ cm^{-1}$, $b_{F,\delta}=-0.0042\ cm^{-1}$, and $b_{F,6s}=0.2577\ cm^{-1}$.[53] Assuming the $X\,^3\Delta_3$ state is a pure state corresponding to the $4\delta^3 16\sigma^1$ electronic configuration, and further assuming that the 16σ orbital has pure Os $6s$ character, these parameters combine to predict $h(X\,^3\Delta_3)=0.149\ cm^{-1}$. This result is completely dominated by the large value of the Fermi contact interaction for the $6s$ electron, $b_{F,6s}$, which alone contributes $0.129\ cm^{-1}$ to the value of h.

Although the hyperfine splitting is not well resolved in any of our spectra, we have attempted to extract values of h'' and h' for all of the bands originating from the $X\,^3\Delta_3$ level by fitting the spectra of the $^{189}Os^{12}C$ isotopomer using the PGOPHER program.[54] To obtain a fit, the experimental spectrum was overlaid on a simulated spectrum, and the hyperfine parameters were varied until the two spectra were similar. Then, specific hyperlines in the experimental spectrum were assigned to the lines in the simulated spectrum, and a least-squares fit was performed. Due to the poor resolution of hyperfine structure in our experiments, the resulting fits are not as definitive as we would like, but good agreement is found among the four fitted bands for the value of $h(X\,^3\Delta_3)$, with values ranging between 0.1287 and $0.1428\ cm^{-1}$. These values are close to the value of $h=0.149\ cm^{-1}$ that is predicted assuming that the 16σ orbital is purely Os $6s$ in character. Assuming that the only effect of admixtures of other atomic orbitals into the 16σ orbital is to reduce the contribution of $b_{F,6s}$ proportionately, these values suggest that the 16σ orbital is approximately 84%–95% $6s$ in character. A more precise interpretation of the hyperfine interactions in this molecule will require investigation at higher resolution. Table III provides a summary of the fit results for the $^{189}Os^{12}C$ isotopomer including hyperfine interactions. Figure 5 presents a comparison of the measured and fitted spectra of the 0-0 band of the $[19.1]2\leftarrow X\,^3\Delta_3$ system of $^{189}Os^{12}C$, including hyperfine effects.

6. The bond length of the $X\,^3\Delta$ state of OsC: Correction for spin-uncoupling effects

To obtain the most accurate estimate of the ground state bond length of OsC, one must take into account the effects of the spin-uncoupling operator, which couples the observed $^3\Delta_3$ ground level to the unobserved $^3\Delta_2$ level. The spin-uncoupling operator affects the magnitude of the rotational constant, such that the measured B value of the $^3\Delta_3$ level is reduced, giving an effective B value that obeys the expression[55]

$$B_{\rm eff}(\Omega)=B_{\rm true}\left(1+\frac{2B_{\rm true}\Sigma}{A\Lambda}\right). \tag{3.8}$$

For the $\delta^3\sigma^1$, $^3\Delta$ ground term of OsC, the spin-orbit parameter A may be estimated using the semiempirical method of Ishiguro and Kobori,[56] providing

$$A=-\zeta_{\rm Os}(5d)/2, \tag{3.9}$$

where the atomic spin-orbit constant $\zeta_{\rm Os}(5d)=3045\ cm^{-1}$ is taken from the compilation of Lefebvre-Brion and Field.[51] After combining the data for all of the OsC isotopomers and correcting for the effects of spin uncoupling, our best estimate of the OsC ground state bond length r_0'' is $1.672\,14\pm0.000\,28$ Å (1σ error limit). The correction for the effects of the spin-uncoupling operator is minor, shortening the estimate of the bond length by only about 0.0003 Å.

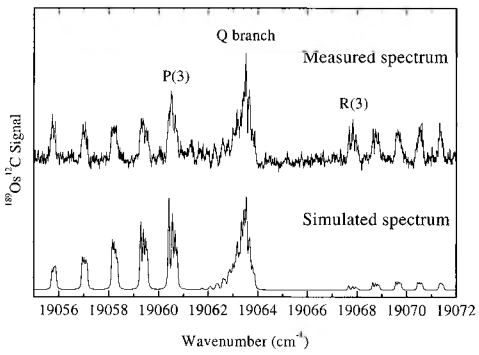

FIG. 5. Measured and simulated spectra of the 0-0 band of the $[19.1]2\leftarrow X\,^3\Delta_3$ system of $^{189}Os^{12}C$, showing hyperfine structure.

Author complimentary copy. Redistribution subject to AIP license or copyright, see http://jcp.aip.org/jcp/copyright.jsp

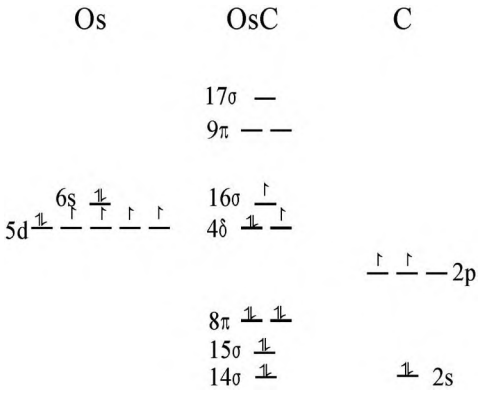

FIG. 6. Qualitative molecular orbital diagram of OsC.

This is due to the small value of B, combined with the large value of A.

IV. DISCUSSION

In considering the possible ground and low-lying electronic states of OsC, it is useful to think about the molecular orbitals of the molecule. The valence atomic orbitals and the molecular orbitals generated from them are displayed in the qualitative molecular orbital diagram of Fig. 6. In this diagram, the 14σ orbital of OsC is assumed to be corelike and mainly carbon $2s$ in character. The 15σ and 17σ orbitals are considered to be bonding and antibonding combinations of the Os $5d\sigma$ and C $2p\sigma$ orbitals, respectively, and the 8π and 9π orbitals are likewise considered to be bonding and antibonding combinations of the Os $5d\pi$ and C $2p\pi$ orbitals. The 16σ orbital is expected to be primarily nonbonding in character, arising from the $6s$ orbital of Os. This is confirmed by the hyperfine measurements described in Sec. III B 5 above. The 4δ orbitals are nonbonding and almost entirely Os $5d\delta$ in character. It is possible that there is significant sp hybridization on the carbon atom, but this possibility has no consequences for the spectroscopic results presented here and will not be discussed further.

Given that OsC has 12 valence electrons, the low-lying 14σ, 15σ, and 8π orbitals are expected to be filled in any low-lying electronic states. The real issue in this molecule concerns how the remaining four electrons fill the 4δ and 16σ orbitals. There are three configurational candidates for the ground electronic state: $4\delta^4$, giving a $^1\Sigma^+$ ground state, as in the isovalent RuC molecule,[37] $4\delta^3 16\sigma^1$, giving a $^3\Delta_3$ ground state, as in the isovalent FeC molecule,[31–33] and $4\delta^2 16\sigma^2$, giving a $^3\Sigma^-$ ($\Omega=0^+$) ground state, as predicted by *ab initio* theory.[16,30] Of these possibilities, only the $^3\Delta_3$ state is consistent with the value of Ω'' obtained from the rotational analyses of the strong bands measured in this work. Therefore, $^3\Delta_3$ is established as the ground state of the OsC molecule.

The other low-lying electronic state observed in this work is a state with $\Omega''=0$. Although there is no experimental evidence that this state has $\Omega=0^+$ parity, the only reasonable electronic configurations that can lead to a low-lying $\Omega=0$ level are the $4\delta^4$, $^1\Sigma^+$ term and the $4\delta^2 16\sigma^2$, $^3\Sigma^-$ term. To distinguish between these possibilities, it is useful to compare the bond lengths expected for the various configurations. In FeC and RuC, transfer of electrons from the δ orbital to the σ orbital leads to an increase in bond length. For example, first-order configuration interaction calculations on RuC predict bond lengths of 1.642 Å (δ^4, $^1\Sigma^+$); 1.666 Å ($\delta^3\sigma^1$, $^3\Delta$), and 1.724 Å ($\delta^2\sigma^2$, $^3\Sigma^-$).[57] The increase in bond length for RuC that accompanies transfer of electrons from the δ to the σ orbital is in agreement with the experimentally measured increase in bond length in going from the δ^4, $^1\Sigma^+$ state (1.608 Å) to the $\delta^3\sigma^1$, $^3\Delta$ state (1.635 Å).[37] Similarly, multireference configuration interaction calculations on the $\delta^3\sigma^1$, $^3\Delta$ ground state of FeC predict a shorter bond length (1.585 Å) than is predicted for the $\delta^2\sigma^2$, $^3\Sigma^-$ state (1.672 Å).[58] Finally, a CCSD(T) calculation on OsC predicts an increase in bond length of 0.02 Å when one shifts an electron from the 4δ orbital to the 16σ orbital, in going from the $4\delta^3 16\sigma^1$, $^3\Delta_3$ term (1.69 Å) to the $4\delta^2 16\sigma^2$, $^3\Sigma^-$ term (1.71 Å). Considering the measured rotational constants for OsC, and the bond lengths that they imply, the increase in bond length of 0.025 Å in going from the $X\ ^3\Delta_3$ level to the low-lying $\Omega=0$ level strongly suggests that this low-lying $\Omega=0$ level arises from the $4\delta^2 16\sigma^2$, $^3\Sigma^-$ term. The fact that this term is predicted to be the ground term in the two published calculations lends credence to this possibility,[16,30] and therefore we assign this low-lying electronic state as the $4\delta^2 16\sigma^2$, $A\ ^3\Sigma^-_{0+}$ level.

The *ab initio* calculations predict that the OsC ground state is the $4\delta^2 16\sigma^2$, $^3\Sigma^-$ term, with the $4\delta^3 16\sigma^1$, $^3\Delta$ term lying 2200 cm^{-1} higher in energy.[16] Adding spin-orbit effects, the $^3\Delta_3$ level is expected to be stabilized in first-order perturbation theory by an amount given by ζ_{5d}(Os), which is about 3045 cm^{-1}. The $4\delta^2 16\sigma^2$, $^3\Sigma^-_{0+}$ level is perturbed by spin-orbit interaction with the higher-lying $4\delta^2 16\sigma^2$, $^1\Sigma^+_{0+}$ level, with which it has a Hamiltonian matrix element given by $\langle 4\delta^2 16\sigma^2, {}^3\Sigma^-_{0+}|\hat{H}^{SO}|4\delta^2 16\sigma^2, {}^1\Sigma^+_{0+}\rangle = 2\zeta_{5d}$(Os). For zeroth-order separations between the $^3\Sigma^-$ and $^1\Sigma^+$ terms of 0–5000 cm^{-1}, this results in a stabilization of the $4\delta^2 16\sigma^2$, $^3\Sigma^-_{0+}$ level by 4000–6000 cm^{-1}. For a zeroth-order separation that is even as large as 10 000 cm^{-1}, the $4\delta^2 16\sigma^2$, $^3\Sigma^-_{0+}$ level is still stabilized by 2880 cm^{-1}. Based on these results, it seems that spin-orbit effects will stabilize the $^3\Sigma^-_{0+}$ level even more than the $^3\Delta_3$ level. Thus, it seems that spin-orbit effects are not sufficient to reverse the predicted energetic ordering of the states to bring them into agreement with experiment. The OsC molecule represents a formidable challenge to quantum chemistry, requiring accurate treatments of electron correlation as well as relativistic effects, including spin-orbit interactions.

The upper states of the spectroscopic transitions reported here consist of the two $\Omega'=2$ states at 19 064 and 21 284 cm^{-1}, an $\Omega'=3$ state at 20 543 cm^{-1}, and two $\Omega'=1$ states at $20\,729+x$ and $21\,006+x$ cm^{-1}, where x represents the energy of the $A\ ^3\Sigma^-_{0+}$ level relative to the $X\ ^3\Delta_3$ ground level. These cannot arise from the low energy configurations of $4\delta^3 16\sigma^1$, $4\delta^2 16\sigma^2$, or $4\delta^2$ because all of the $\Omega=1$, 2, or 3 levels arising from these configurations are expected to be within about 6000 cm^{-1} of the $X\ ^3\Delta_3$ or $A\ ^3\Sigma^-_{0+}$ levels. Thus, the upper levels involved in the measured transitions must involve either promotion of an electron from the 8π or 15σ

Author complimentary copy. Redistribution subject to AIP license or copyright, see http://jcp.aip.org/jcp/copyright.jsp

bonding orbitals into the nonbonding 4δ and 16σ orbitals or promotion of an electron from the nonbonding 4δ and 16σ orbitals into the antibonding 9π and 17σ orbitals. In the case of RuC, electronic states lying in the range from 12 700 to 18 100 cm^{-1} could be confidently assigned to the $2\delta^3 6\pi^1$ configuration, which corresponds to the $4\delta^3 9\pi^1$ configuration of OsC. This configuration generates two $\Omega'=3$ levels ($^3\Phi_3$ and $^1\Phi_3$), two $\Omega=2$ levels ($^3\Phi_2$ and $^3\Pi_2$), and two $\Omega'=1$ levels ($^1\Pi_1$ and $^3\Pi_1$), although these are expected to be very strongly mixed by spin-orbit effects due to the large spin-orbit parameter of Os. Given the stabilization of the 16σ orbital in OsC, however, it is more likely that the upper states of these transitions correspond to the $4\delta^2 16\sigma^1 9\pi^1$ configuration, which generates three $\Omega=3$ levels ($^1\Phi_3$, $^3\Phi_3$, and $^5\Pi_3$), five $\Omega=2$ levels (three $^3\Pi_2$, one $^5\Pi_2$, and one $^3\Phi_2$ level), and six $\Omega=1$ levels (two $^1\Pi_1$, three $^3\Pi_1$, and one $^5\Pi_1$ level). Without additional information, such as might be obtained by a study of OsC in the red region of the spectrum or dispersed fluorescence studies, or by a more detailed computational investigation, it is impossible to identify either the upper state configurations or term symbols for this molecule.

Even though the spectroscopic data on the $5d$ transition metal carbides are limited to WC,[1,2] IrC,[3–5] PtC,[7,8,11,13] and now OsC, it is clear that in these molecule states in which the $6s$-like 16σ orbital is occupied are stabilized. For example, the ground level of WC is $4\delta^1 16\sigma^1$, $^3\Delta_1$,[1] as compared to the $2\delta^2$, $^3\Sigma^-_{0+}$ ground level of MoC.[59] Similarly, the ground level of IrC is $4\delta^3 16\sigma^2$, $^2\Delta_{5/2}$,[3,4,27] as compared to the $2\delta^4 9\sigma^1$, $^2\Sigma^+$ ground level of RhC.[60–63] Our newly recorded data on OsC fit nicely into this trend: OsC has a $4\delta^3 16\sigma^1$, $^3\Delta_3$ ground term, while RuC has a $2\delta^4$, $^1\Sigma^+$ ground term.[37] These results reflect the relativistic stabilization of the $6s$ orbital, an effect that is responsible for the yellow color of metallic gold, the fact that mercury is a liquid at room temperature, and the "inert pair effect," in which the more stable oxidation states of thallium (Tl^{1+}), lead (Pb^{2+}), and bismuth (Bi^{3+}) retain two electrons in the $6s$ orbital.[64]

V. CONCLUSION

The electronic spectrum of diatomic OsC was recorded in the range from 17 390 to 22 990 cm^{-1}, using resonant two-photon ionization spectroscopy. This study reveals that the ground term of OsC is $4\delta^3 16\sigma^1$, $X\ ^3\Delta_3$ and that the $4\delta^2 16\sigma^2$, $A\ ^3\Sigma^-_{0+}$ level lies low enough in energy to be populated in the jet-cooled molecular beam. Rotational constants and bond lengths are reported for these states and for six excited vibronic levels of diatomic OsC.

ACKNOWLEDGMENTS

The authors thank the U.S. Department of Energy for support of this research under Grant No. DE-FG03-01ER15176.

[1] S. M. Sickafoose, A. W. Smith, and M. D. Morse, J. Chem. Phys. **116**, 993 (2002).
[2] X. Li, S. S. Liu, W. Chen, and L.-S. Wang, J. Chem. Phys. **111**, 2464 (1999).
[3] K. Jansson, R. Scullman, and B. Yttermo, Chem. Phys. Lett. **4**, 188 (1969).
[4] K. Jansson and R. Scullman, J. Mol. Spectrosc. **36**, 248 (1970).
[5] A. J. Marr, M. E. Flores, and T. C. Steimle, J. Chem. Phys. **104**, 8183 (1996).
[6] T. Ma, J. W. H. Leung, and A. S. C. Cheung, Chem. Phys. Lett. **385**, 259 (2004).
[7] H. Neuhaus, R. Scullman, and B. Yttermo, Z. Naturforsch. A **20A**, 162 (1965).
[8] R. Scullman and B. Yttermo, Ark. Fys. **33**, 231 (1966).
[9] O. Appelblad, R. F. Barrow, and R. Scullman, Proc. Phys. Soc. London **91**, 260 (1967).
[10] O. Appelblad, C. Nilsson, and R. Scullman, Phys. Scr. **7**, 65 (1973).
[11] T. C. Steimle, K. Y. Jung, and B.-Z. Li, J. Chem. Phys. **102**, 5937 (1995).
[12] T. C. Steimle, K. Y. Jung, and B.-Z. Li, J. Chem. Phys. **103**, 1767 (1995).
[13] S. A. Beaton and T. C. Steimle, J. Chem. Phys. **111**, 10876 (1999).
[14] T. C. Steimle, M. L. Costen, G. E. Hall, and T. J. Sears, Chem. Phys. Lett. **319**, 363 (2000).
[15] K. A. Gingerich and D. L. Cocke, Inorg. Chim. Acta **28**, L171 (1978).
[16] G. Meloni, L. M. Thomson, and K. A. Gingerich, J. Chem. Phys. **115**, 4496 (2001).
[17] N. S. McIntyre, A. Vander Auwera-Mahieu, and J. Drowart, Trans. Faraday Soc. **64**, 3006 (1968).
[18] S. K. Gupta, B. M. Nappi, and K. A. Gingerich, J. Phys. Chem. **85**, 971 (1981).
[19] A. V. Auwera-Mahieu and J. Drowart, Chem. Phys. Lett. **1**, 311 (1967).
[20] F. J. Kohl and C. A. Stearns, High. Temp. Sci. **6**, 284 (1974).
[21] P. B. Armentrout, S. Shin, and R. Liyanage, J. Phys. Chem. A **110**, 1242 (2006).
[22] M. M. Armentrout, F.-X. Li, and P. B. Armentrout, J. Phys. Chem. A **108**, 9660 (2004).
[23] F.-X. Li, X.-G. Zhang, and P. B. Armentrout, Int. J. Mass. Spectrom. **255–256**, 279 (2006).
[24] X.-G. Zhang, R. Liyanage, and P. B. Armentrout, J. Am. Chem. Soc. **123**, 5563 (2001).
[25] D. Majumdar and K. Balasubramanian, Chem. Phys. Lett. **284**, 273 (1998).
[26] K. Balasubramanian, J. Chem. Phys. **112**, 7425 (2000).
[27] H. Tan, M. Liao, and K. Balasubramanian, Chem. Phys. Lett. **280**, 219 (1997).
[28] B. F. Minaev, Phys. Chem. Chem. Phys. **2**, 2851 (2000).
[29] M. Barysz and P. Pyykko, Chem. Phys. Lett. **285**, 398 (1998).
[30] J. Wang, X. Sun, and Z. Wu, J. Cluster Sci. **18**, 333 (2007).
[31] W. J. Balfour, J. Cao, C. V. V. Prasad, and C. X. Qian, J. Chem. Phys. **103**, 4046 (1995).
[32] M. D. Allen, T. C. Pesch, and L. M. Ziurys, Astrophys. J. **472**, L57 (1996).
[33] D. J. Brugh and M. D. Morse, J. Chem. Phys. **107**, 9772 (1997).
[34] K. Aiuchi, K. Tsuji, and K. Shibuya, Chem. Phys. Lett. **309**, 229 (1999).
[35] R. Scullman and B. Thelin, Phys. Scr. **3**, 19 (1971).
[36] R. Scullman and B. Thelin, Phys. Scr. **5**, 201 (1972).
[37] J. D. Langenberg, R. S. DaBell, L. Shao, D. Dreessen, and M. D. Morse, J. Chem. Phys. **109**, 7863 (1998).
[38] R. S. DaBell, R. G. Meyer, and M. D. Morse, J. Chem. Phys. **114**, 2938 (2001).
[39] N. F. Lindholm, D. A. Hales, L. A. Ober, and M. D. Morse, J. Chem. Phys. **121**, 6855 (2004).
[40] W. C. Wiley and I. H. McLaren, Rev. Sci. Instrum. **26**, 1150 (1955).
[41] B. A. Mamyrin, V. I. Karataev, D. V. Shmikk, and V. A. Zagulin, Zh. Eksp. Teor. Fiz. **64**, 82 (1973).
[42] S. Gerstenkorn and P. Luc, *Atlas du Spectre d'Absorption de la Molécule d' Iode entre* 14,800–20,000 cm^{-1} (CNRS, Paris, 1978).
[43] S. Gerstenkorn and P. Luc, Rev. Phys. Appl. **14**, 791 (1979).
[44] J. Cariou and P. Luc, *Atlas du Spectre d'Absorption de la Molécule Tellure, Partie 5:* 21,100–23,800 cm^{-1} (CNRS, Paris, 1980).
[45] J. Cariou and P. Luc, *Atlas du Spectre d'Absorption de la Molécule de Tellure entre* 18,500–23,800 cm^{-1} (CNRS, Paris, 1980).
[46] P. R. Bevington, *Data Reduction and Error Analysis for the Physical Sciences* (McGraw-Hill, New York, 1969).
[47] See EPAPS Document No. E-JCPSA6-128-041803 for 18 pages of line positions, rotational fits, and rotationally resolved spectra of OsC. The document can be reached through a direct link in the online article's HTML reference section or via the EPAPS homepage (http://www.aip.org/pubservs/epaps.html).
[48] I. Kopp and J. T. Hougen, Can. J. Phys. **45**, 2581 (1967).

Author complimentary copy. Redistribution subject to AIP license or copyright, see http://jcp.aip.org/jcp/copyright.jsp

[49] T. M. Dunn, in *Molecular Spectroscopy: Modern Research*, edited by K. N. Rao and C. W. Mathews (Academic, New York, 1972), pp. 231–57.
[50] W. Weltner, Jr., *Magnetic Atoms and Molecules* (Dover, New York, 1983).
[51] H. Lefebvre-Brion and R. W. Field, *The Spectra and Dynamics of Diatomic Molecules* (Elsevier, Amsterdam, 2004).
[52] C. H. Townes and A. L. Schawlow, *Microwave Spectroscopy* (Dover, New York, 1975).
[53] S. Büttgenbach, *Hyperfine Structure in 4d- and 5d-Shell Atoms* (Springer-Verlag, Berlin, 1982).
[54] C. M. Western, PGOPHER, a Program for Simulating Rotational Structure, University of Bristol, http://pgopher.chm.bris.ac.uk.
[55] G. Herzberg, *Molecular Spectra and Molecular Structure I. Spectra of Diatomic Molecules*, 2nd ed. (Van Nostrand Reinhold, New York, 1950).
[56] E. Ishiguro and M. Kobori, J. Phys. Soc. Jpn. **22**, 263 (1967).
[57] R. Guo and K. J. Balasubramanian, J. Chem. Phys. **120**, 7418 (2004).
[58] D. Tzeli and A. Mavridis, J. Chem. Phys. **116**, 4901 (2002).
[59] D. J. Brugh, T. J. Ronningen, and M. D. Morse, J. Chem. Phys. **109**, 7851 (1998).
[60] A. Lagerqvist and R. Scullman, Ark. Fys. **32**, 475 (1966).
[61] B. Kaving and R. Scullman, J. Mol. Spectrosc. **32**, 475 (1969).
[62] J. M. Brom, Jr., W. R. M. Graham, and W. Weltner, Jr., J. Chem. Phys. **57**, 4116 (1972).
[63] W. J. Balfour, S. G. Fougère, R. F. Heuff, C. X. W. Qian, and C. Zhou, J. Mol. Spectrosc. **198**, 393 (1999).
[64] K. Balasubramanian, J. Phys. Chem. **93**, 6585 (1989).

Author complimentary copy. Redistribution subject to AIP license or copyright, see http://jcp.aip.org/jcp/copyright.jsp